Nuclear Physics A443 (1985) 365–379

ON THE IMAGINARY PART OF THE FORM FACTOR FOR INELASTIC EXCITATIONS IN HEAVY-ION REACTIONS

C.H. DASSO and G. POLLAROLO*

The Niels Bohr Institute and Nordita, Blegdamsvej 17, DK-2100 Copenhagen Ø, Denmark

and

S. LANDOWNE**

Technische Universität München, D-8046 Garching, West Germany

Received 20 March 1985

Abstract: An explicit formula is obtained for the imaginary inelastic transition form factor which accounts for second-order excitation processes. The transfer of nucleons back and forth between projectile and target is found to be the leading higher-order effect. This result and the close connection which is obtained between the imaginary form factor and the absorptive part of the optical potential explains the main features of the macroscopic prescription commonly used in data analyses.

1. Introduction

In this work we examine the nature of the effective coupling interaction for heavy-ion inelastic scattering. Our main interest here is to obtain a better understanding of the imaginary part of this interaction and to provide a means for calculating it microscopically. While microscopic calculations have been successful in constructing the real part of the form factors [see e.g. ref. [1])] no comparable effort has been devoted to identifying the origin or to estimating the magnitude of the imaginary component. In this sense we consider the subject covered in this paper as a natural extension of the developments reported in ref. [1]). We note that the complex character of the effective coupling is essential to obtain a satisfactory account of the observed inelastic cross sections in terms of DWBA calculations. The familiar macroscopic prescription which relates the imaginary inelastic coupling interaction to the derivative of the elastic absorption potential has been extensively used in data analyses. As we shall see, it is possible to recover the main physical features of the conventional procedure but only by identifying higher-order transfer reactions as the main source of the imaginary coupling.

* Permanent address: Istituto di Fisica Teorica dell' Universita di Torino and INFN, Sezione di Torino, Torino, Italy.

** Supported by a grant from the Bundesministerium für Forschung und Technologie, Federal Republic of Germany.

We shall study in detail transitions involving two single-particle states of the target nucleus. The results of this analysis apply directly to the description of inelastic excitations in odd systems. They can also be elaborated further to construct the effective coupling interactions for collective surface modes in the case of even nuclei. In sect. 2 we use semiclassical theory to obtain an explicit expression for the effective interaction for single-particle transitions in terms of one-step inelastic and two-step inelastic and transfer processes. The extension of the formalism for collective surface modes is also discussed here. The basic structure of the resulting form factors is analyzed in sect. 3 while illustrative numerical calculations are given in sect. 4. Finally, sect. 5 summarizes our conclusions.

2. Semiclassical formulation of the effective interaction

2.1. SINGLE-PARTICLE TRANSITIONS

Consider a collision between two heavy nuclei where an inelastic excitation between two shell-model states $\alpha \to \beta$ occurs in one of the reaction partners due to the interaction V. The amplitude for this process is given in first-order semiclassical perturbation theory by

$$c_{\beta\alpha}^{(1)} = (-i/\hbar)\int_{-\infty}^{\infty} \mathrm{d}t \langle j_\beta m_\beta | V(\boldsymbol{r}(t)) | j_\alpha m_\alpha \rangle \, \mathrm{e}^{i\omega_{\beta\alpha}t},$$

where $\boldsymbol{r}(t)$ is the trajectory of relative motion and $\hbar\omega_{\beta\alpha} = E_\beta - E_\alpha$ is the energy difference between the final and initial states. The corresponding second-order contribution is

$$c_{\beta\alpha}^{(2)} = (-1/\hbar^2)\sum_\gamma \int_{-\infty}^{\infty} \mathrm{d}t \langle j_\beta m_\beta | V(\boldsymbol{r}(t)) | j_\gamma m_\gamma \rangle \, \mathrm{e}^{i\omega_{\beta\gamma}t}$$

$$\times \int_{-\infty}^{t} \mathrm{d}t' \langle j_\gamma m_\gamma | V(\boldsymbol{r}(t')) | j_\alpha m_\alpha \rangle \, \mathrm{e}^{i\omega_{\gamma\alpha}t'}.$$

Our strategy is to recast $c_{\beta\alpha}^{(2)}$ into the same form as $c_{\beta\alpha}^{(1)}$ and thereby obtain an effective first-order interaction which accounts for the second-order processes.

Notice that in the product space of the two reacting fragments these processes are either two-step inelastic transitions within the nucleus which is excited or two-step transfer reactions which go back and forth between the collision partners. We will be assuming the "no-recoil" approximation so that transfer couplings have the same form as inelastic transitions. It should be kept in mind, however, that transfer form factors are longer-ranged than the form factors for inelastic excitations.

To proceed we introduce radial form factors through the multipole expansion

$$\langle j_\beta m_\beta | V(\boldsymbol{r}) | j_\alpha m_\alpha \rangle = \sum_{\lambda\mu} \left[(-)^{\lambda+\mu}/\hat{\lambda}\right] (j_\alpha m_\alpha \lambda - \mu | j_\beta m_\beta) f_\lambda^{\beta\alpha}(r) Y_{\lambda\mu}(\hat{\boldsymbol{r}}),$$

and use the focal coordinate system[2]) where the z-axis is perpendicular to the plane

of the orbit and the x-axis bisects the trajectory. This allows us to write

$$Y_{\lambda\mu}(\hat{r}(t)) = Y_{\lambda\mu}(\tfrac{1}{2}\pi, 0)\, e^{i\mu\phi(t)}.$$

We shall also simplify the discussion by considering a backward scattering trajectory where $\phi(t) \simeq 0$ throughout the motion. This limit is appropriate for investigating the radial dependence of the effective interaction. After a straightforward calculation one obtains

$$c^{(1)}_{\beta\alpha} + c^{(2)}_{\beta\alpha} = \sum_{\lambda\mu} \left[(-)^{\lambda+\mu}/\hat{\lambda}\right] (j_\alpha m_\alpha \lambda - \mu | j_\beta m_\beta) Y_{\lambda\mu}(\tfrac{1}{2}\pi, 0)$$
$$\times \left\{ -iI_{\beta\alpha}(\omega_{\beta\alpha}) - \sum_{\gamma} \sum_{\lambda_\beta \lambda_\alpha} (\hat{\lambda}\hat{j}_\gamma/\sqrt{4\pi})(\lambda_\alpha 0 \lambda_\beta 0 | \lambda 0) \right.$$
$$\left. \times W(j_\alpha \lambda_\alpha j_\beta \lambda_\beta; j_\gamma \lambda) I_{\beta\gamma\alpha}(\omega_{\beta\gamma}, \omega_{\gamma\alpha}) \right\},$$

where the first and second-order orbital integrals are given by

$$I_{\beta\alpha}(\omega_{\beta\alpha}) = (1/\hbar) \int_{-\infty}^{\infty} dt f^{\beta\alpha}_{\lambda}(r(t))\, e^{i\omega_{\beta\alpha} t},$$

$$I_{\beta\gamma\alpha}(\omega_{\beta\gamma}, \omega_{\gamma\alpha}) = (1/\hbar^2) \int_{-\infty}^{\infty} dt f^{\beta\gamma}_{\lambda_\beta}(r(t))\, e^{i\omega_{\beta\gamma} t}$$
$$\times \int_{-\infty}^{t} dt' f^{\gamma\alpha}_{\lambda_\alpha}(r(t'))\, e^{i\omega_{\gamma\alpha} t'}.$$

Notice that $I_{\beta\alpha}$ is a purely real number. The real and imaginary parts of $I_{\beta\gamma\alpha}$ can be separated using the principal value integral

$$(i/\pi) \mathrm{P} \int_{-\infty}^{\infty} (dq/q)\, e^{-iq(t-t')} = \begin{cases} -1 & t > t' \\ +1 & t < t', \end{cases}$$

as was done in ref. [2]) for second-order Coulomb excitation processes. In this way one finds

$$\mathrm{Re}\, I_{\beta\gamma\alpha} = \tfrac{1}{2} I_{\beta\gamma}(\omega_{\beta\gamma}) I_{\gamma\alpha}(\omega_{\gamma\alpha}),$$

$$\mathrm{Im}\, I_{\beta\gamma\alpha} = \frac{1}{2\pi} \mathrm{P} \int_{-\infty}^{\infty} (dq/q) I_{\beta\gamma}(\omega_{\beta\gamma} - q) I_{\gamma\alpha}(\omega_{\gamma\alpha} + q).$$

The real and imaginary parts of $I_{\beta\gamma\alpha}$ give rise to imaginary and real effective form factors, respectively, when $I_{\beta\gamma\alpha}$ is brought to the same form as $I_{\beta\alpha}$.

To achieve this we follow a line of argument similar to the one used in ref. [3]) to localize the imaginary part of the optical potential. We assume that $r(t)$ can be approximated by a parabolic trajectory around the distance of closest approach,

$$r(t) \simeq r_0 + \tfrac{1}{2} \ddot{r}_0 t^2,$$

and that the radial form factors can be parametrized by decaying exponentials,

$$f^{\beta\alpha}_{\lambda}(r(t)) \simeq f^{\beta\alpha}_{\lambda}(r_0) \exp\left[-\ddot{r}_0 t^2 / 2a_{\beta\alpha} \right].$$

We thus obtain

$$I_{\beta\alpha}(\omega_{\beta\alpha}) = (1/\hbar) f_{\lambda}^{\beta\alpha}(r_0)\sqrt{2\pi a_{\beta\alpha}/\ddot{r}_0}\exp\left[-\omega_{\beta\alpha}^2 a_{\beta\alpha}/2\ddot{r}_0\right],$$

and $I_{\beta\gamma\alpha}$ becomes proportional to the product $f_{\lambda_\beta}^{\beta\gamma}(r_0) f_{\lambda_\alpha}^{\gamma\alpha}(r_0)$. By applying the same reasoning we can make the identity

$$f_{\lambda_\beta}^{\beta\gamma}(r_0) f_{\lambda_\alpha}^{\gamma\alpha}(r_0) = \int_{-\infty}^{\infty} \mathrm{d}t f_{\lambda_\beta}^{\beta\gamma}(r) f_{\lambda_\alpha}^{\gamma\alpha}(r)\, \mathrm{e}^{i\omega_{\beta\alpha}t}\sqrt{\ddot{r}_0/2\pi\bar{a}}\exp\left[\omega_{\beta\alpha}^2\bar{a}/2\ddot{r}_0\right],$$

where $\bar{a} = a_{\beta\gamma}a_{\gamma\alpha}/(a_{\beta\gamma} + a_{\gamma\alpha})$. In this way we obtain

$$I_{\beta\gamma\alpha} = (1/2\hbar^2)\int_{-\infty}^{\infty} \mathrm{d}t f_{\lambda_\beta}^{\beta\gamma} f_{\lambda_\alpha}^{\gamma\alpha}\, \mathrm{e}^{i\omega_{\beta\alpha}t}\sqrt{2\pi(a_{\beta\gamma} + a_{\gamma\alpha})/\ddot{r}_0}$$

$$\times\left\{\exp\left[-\frac{(\omega_{\gamma\alpha}a_{\gamma\alpha} - \omega_{\beta\gamma}a_{\beta\gamma})^2}{2\ddot{r}_0(a_{\gamma\alpha} + a_{\beta\gamma})}\right]\right.$$

$$\left. + (i/\pi)\mathrm{P}\int_{-\infty}^{\infty}(\mathrm{d}q/q)\exp\left[-\left(q + \frac{\omega_{\gamma\alpha}a_{\gamma\alpha} - \omega_{\beta\gamma}a_{\beta\gamma}}{a_{\gamma\alpha} + a_{\beta\gamma}}\right)^2\frac{a_{\gamma\alpha} + a_{\beta\gamma}}{2\ddot{r}_0}\right]\right\}.$$

Notice how the last factor in braces depends only on the difference $\omega_{\gamma\alpha}a_{\gamma\alpha} - \omega_{\beta\gamma}a_{\beta\gamma}$.

Using this result we finally obtain the following expression for the imaginary part of the effective single-particle transition form factor:

$$\mathrm{Im}\,\tilde{f}_{\lambda}^{\beta\alpha}(r) = -\frac{1}{2}\sum_{\gamma}\sum_{\lambda_\beta\lambda_\alpha}\hat{\lambda}\hat{j}_\gamma(\lambda_\alpha 0\lambda_\beta 0|\lambda 0)W(j_\alpha\lambda_\alpha j_\beta\lambda_\beta; j_\gamma\lambda)$$

$$\times f_{\lambda_\beta}^{\beta\gamma}(r) f_{\lambda_\alpha}^{\gamma\alpha}(r)\left[(a_{\beta\gamma} + a_{\gamma\alpha})/2\hbar^2\ddot{r}_0\right]^{1/2}$$

$$\times\exp\left[-\frac{(\omega_{\gamma\alpha}a_{\gamma\alpha} - \omega_{\beta\gamma}a_{\beta\gamma})^2}{2\ddot{r}_0(a_{\beta\gamma} + a_{\gamma\alpha})}\right].$$

The corresponding correction to the real form factor is obtained by changing the sign of this expression and replacing the exponential factor by the principal integral in the preceding equation. These expressions will be evaluated in sect. 4 using form factors for single-particle inelastic excitation and single-particle transfer reactions.

2.2. EXTENSION TO COLLECTIVE SURFACE MODES

At this point we have derived in detail the expressions for the effective interaction coupling for a transition between two shell-model states $\alpha \to \beta$. Thus the results

apply directly to the case of inelastic excitation of a system with a nucleon outside a closed shell, such as ^{209}Pb. If we consider the closed-shell nucleus itself at the level of the independent-particle model, the excited states are given by particle-hole configurations. The generalization for this kind of processes is straightforward, as the matrix elements connecting $(|p\rangle \rightarrow |p'\rangle)$ and $(|0\rangle \rightarrow |p(p')^{-1}\rangle)$ are related to each other by a simple multiplicative factor.

To extend further to the excitation of collective surface modes in closed-shell nuclei we have to incorporate the effect of the residual interactions. Their presence in the nucleus is responsible for creating a new set of elementary modes of excitation. Within the RPA formalism these states are expressed as a linear superposition of particle-hole excitations. This transformation establishes the basis for performing microscopic calculations of the form factors. It was used to construct the real part of the first-order form factor in ref. [1]). One could calculate the corresponding second-order contribution for each particle-hole component using the formulae obtained above. However one should expect in the case of collective excitations that the summation over the many components will average out the part which comes from inelastic transitions. Second-order particle-hole transitions can not interfere with a one-phonon excitation in the limit of purely harmonic vibrations. It may be noted that when the vibrational model is taken to all orders in the sudden limit [4]), the range of the resulting imaginary form factor is too short to account for the empirically inferred values.

Retaining only intermediate transitions associated with particle transfer has an interesting practical advantage. The formalism used in ref. [1]) can then be generalized to produce the imaginary part of the form factors simply by allowing the basic building block for single-particle transitions to acquire a complex character. This originates from the second-order transfer terms which can be calculated using the expressions developed in subsect. 2.1. Some examples of these complex kernels will be shown in sect. 4.

3. The structure of the effective interaction

Several interesting features of the effective interaction can be deduced from the structure of the formulae obtained in sect. 2. In order to bring them out clearly it is convenient to neglect angular momentum couplings and use a more condensed notation. We thus consider an analogue problem where the coupling interaction depends only on the radial distance:

$$a_{\beta\alpha}^{(1)} = (-i/\hbar)\int_{-\infty}^{\infty} \mathrm{d}t\, V_{\beta\alpha}[r(t)]\,\mathrm{e}^{i\omega t},$$

$$a_{\beta\alpha}^{(2)} = (-1/\hbar^2)\sum_{\gamma}\int_{-\infty}^{\infty} \mathrm{d}t\, V_{\beta\gamma}(t)\,\mathrm{e}^{i\omega_{\beta\gamma}t}\int_{-\infty}^{t} \mathrm{d}t'\, V_{\gamma\alpha}(t')\,\mathrm{e}^{i\omega_{\gamma\alpha}t'}.$$

Following the discussion in subsect. 2.1 we have

$$a_{\beta\alpha}^{(1)} = (-i/\hbar) V_{\beta\alpha}(r_0) \sqrt{2\pi\sigma^2}\, \mathrm{e}^{-\omega^2\sigma^2/2},$$

$$a_{\beta\alpha}^{(2)} = (-1/\hbar^2) \sum_{\gamma} V_{\beta\gamma}(r_0) V_{\gamma\alpha}(r_0) I_{\gamma}(\omega_{\beta\gamma}, \omega_{\gamma\alpha}),$$

$$I_{\gamma}(\omega_{\beta\gamma}, \omega_{\gamma\alpha}) = \int_{-\infty}^{\infty} \mathrm{d}t\, \mathrm{e}^{[(-t^2/2\sigma_{\gamma}^2) + i\omega_{\beta\gamma} t]} \int_{-\infty}^{t} \mathrm{d}t'\, \mathrm{e}^{[(-t'^2/2\sigma_{\gamma}^2) + i\omega_{\gamma\alpha} t']}.$$

Here we have defined $\sigma^2 \equiv a/\ddot{r}_0$. We have also taken equal decay lengths for the intermediate interactions. Notice that $\omega_{\beta\gamma} + \omega_{\gamma\alpha} = \omega$. Defining the effective coupling by

$$a_{\beta\alpha}^{(1)} + a_{\beta\alpha}^{(2)} = (-i/\hbar) \int_{-\infty}^{\infty} \mathrm{d}t \left(V_{\beta\alpha} + \Delta V_{\beta\alpha} + i W_{\beta\alpha} \right) \mathrm{e}^{i\omega t},$$

we obtain finally

$$W_{\beta\alpha}(r) = -\sum_{\gamma} V_{\beta\gamma}(r) V_{\gamma\alpha}(r) \sqrt{\pi\sigma_{\gamma}^2/\hbar^2}\, \mathrm{e}^{-[(\omega_{\gamma\alpha} - \omega_{\beta\gamma})^2 \sigma_{\gamma}^2/4]},$$

$$\Delta V_{\beta\alpha}(r) = \sum_{\gamma} V_{\beta\gamma}(r) V_{\gamma\alpha}(r) \sqrt{\sigma_{\gamma}^2/\pi\hbar^2}$$

$$\times \mathrm{P} \int_{-\infty}^{\infty} (\mathrm{d}q/q)\, \mathrm{e}^{[-(2q + \omega_{\gamma\alpha} - \omega_{\beta\gamma})^2 \sigma_{\gamma}^2/4]}.$$

It can be seen from these results that at large distances, where the matrix elements are determined by the tails of the single-particle wave functions, each intermediate transition adds constructively to build up the imaginary part of the coupling. The imaginary form factor therefore gives a measure of the number of indirect transitions leading to the final state. The energy-dependent factor in $W_{\beta\alpha}$ favors the contribution from states lying half-way between the initial and final states ($\omega_{\gamma\alpha} = \omega_{\beta\gamma} = \frac{1}{2}\omega$). Notice that for a uniform distribution of the products $V_{\beta\gamma} V_{\gamma\alpha}$ the summation over intermediate states makes $W_{\beta\alpha}$ independent of the total excitation energy. Empirical data analyses have always used imaginary form factors which are independent of the excitation energy but this point has not been investigated critically.

The energy-dependent factor in the correction to the real coupling $\Delta V_{\beta\alpha}$ is an antisymmetric function of the difference $\omega_{\gamma\alpha} - \omega_{\beta\gamma}$, being negative for $\omega_{\gamma\alpha} > \omega_{\beta\gamma}$ and positive for $\omega_{\gamma\alpha} < \omega_{\beta\gamma}$. Thus the states in the intermediate-energy range which can contribute strongly to $W_{\beta\alpha}$ contribute little to $\Delta V_{\beta\alpha}$. The sum over the intermediate states causes $\Delta V_{\beta\alpha}$ to vanish for a uniform distribution of coupling strengths. This condition, however, is unlikely to occur in actual cases. It may be noted that empirical analyses have not isolated a correction to the real form factor.

It is interesting to note that within the present model the imaginary part of the optical potential for elastic scattering[3]) is just given by

$$W_{\alpha\alpha}(r) = -\sum_{\gamma} V_{\alpha\gamma}(r) V_{\gamma\alpha}(r) \sqrt{\pi\sigma_{\gamma}^2/\hbar^2}\, \mathrm{e}^{-\omega_{\gamma\alpha}^2 \sigma_{\gamma}^2}.$$

Clearly $W_{\beta\alpha}$ and $W_{\alpha\alpha}$ have a similar structure, especially when the final excited state lies close to the ground state. The main difference is in the number of terms which contribute. The imaginary potential counts all the channels which couple to the ground state while $W_{\beta\alpha}$ selects from these the ones which also couple to the excited state β. For instance, projectile excitation contributes to $W_{\alpha\alpha}$ but not to $W_{\beta\alpha}$ when β is an excited state of the target. Thus the ratio $W_{\beta\alpha}/W_{\alpha\alpha}$ will be less than one unless there are special cases where $V_{\beta\gamma} \gg V_{\alpha\gamma}$. This ratio should be a constant close to one at large distances where transfer reactions determine the behaviour of the absorption [3]). Empirical analyses support this conclusion.

The usual macroscopic prescription presupposes that the imaginary coupling interaction is proportional to the absorptive part of the optical potential at large distances. Such analyses also often fix the diffuseness of the imaginary form factor to be similar to that of the real coupling. According to the formulae above this can be explained by the fact that the product $V_{\beta\gamma}V_{\gamma\alpha}$ for two transfer reactions decays like an inelastic excitation interaction. This will be illustrated explicitly in the next section.

As a final related point we note that if the real and imaginary interactions $V_{\beta\alpha}, W_{\beta\alpha}$ do have the same shape then we can expect that the phase of the nuclear excitation amplitude should be independent of the excitation energy. It would be interesting to see if this point can be checked by comparing Coulomb-nuclear interference patterns for low-lying quadrupole excitations to those of high-lying giant quadrupole resonances.

4. Numerical calculations

4.1. SINGLE-PARTICLE EXCITATIONS

In this section we present numerical calculations for some illustrative cases. We consider first of all the collision of $^{16}O + ^{209}Pb$ and excite the valence neutron in the $2g_{9/2}$ orbital to the neighboring $1i_{11/2}$ state. We then take into account all the possible two-step inelastic transitions among the valence orbitals of ^{209}Pb and the two-step transfer reactions via the valence orbitals of ^{17}O to obtain the imaginary form factor. Note that this restricted space does not allow for core-polarization effects. The single-particle states which define the space for these calculations are shown in fig. 1. They are generated from typical binding potentials. The corresponding radial wave functions are used to calculate the microscopic inelastic and transfer form factors, as discussed in detail in refs. [1,3]).

The direct transition $2g_{9/2} \rightarrow 1i_{11/2}$ involves orbital angular momentum transfers of $\lambda = 2, 4, 6, 8, 10$. The corresponding radial form factors are plotted in fig. 2. They all have similar magnitudes and shapes over the distances considered. To summarize this information we fit exponentials to the tails of these form factors and refer the

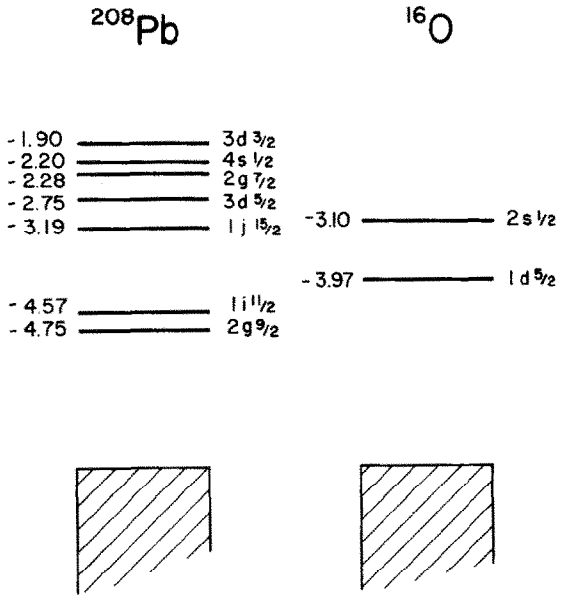

Fig. 1. Neutron particle orbitals outside the closed shells corresponding to ^{208}Pb and ^{16}O.

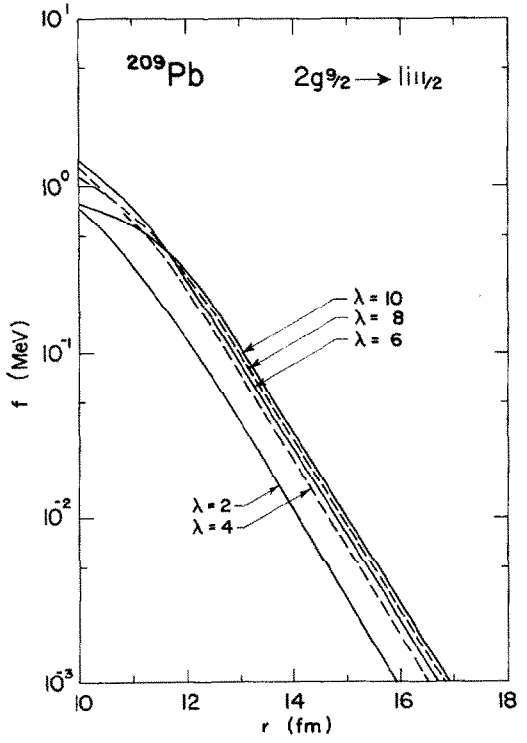

Fig. 2. Direct inelastic excitation form factors for the different multipolarities in the transition $^{209}\mathrm{Pb}(2g_{9/2})(^{16}\mathrm{O},^{16}\mathrm{O}')^{209}\mathrm{Pb}(1i_{11/2})$.

magnitudes to a common radius $R_0 = 1.2(A_1^{1/3} + A_2^{1/3}) = 10.13$ fm so that

$$f_\lambda(r) \to F_0 \exp[-(r - R_0)/a] .$$

We shall also use such parametrized form factors to construct the imaginary coupling. The values of F_0 and a for the $2g_{9/2} \to 1i_{11/2}$ transition followed by those for all of the $2g_{9/2} \to nlj$ and $nlj \to 1i_{11/2}$ transitions within the ^{209}Pb level scheme of

TABLE 1

Strength and diffuseness parameters of single-particle inelastic excitation form factors for ^{209}Pb(^{16}O, ^{16}O′)

Transition	λ	F_0 [MeV]	a [fm]
$2g_{9/2} \to 1i_{11/2}$	10	−7.6	0.76
	8	7.2	0.75
	6	−6.8	0.75
	4	5.2	0.75
	2	−2.8	0.74
$2g_{9/2} \to 1j_{15/2}$	11	2.0	0.76
	9	−4.3	0.76
	7	7.4	0.75
	5	−10.4	0.75
	3	14.4	0.74
$1j_{15/2} \to 1i_{11/2}$	13	1.2	0.74
	11	−2.2	0.73
	9	3.0	0.73
	7	−3.6	0.72
	5	3.7	0.71
	3	−2.5	0.71
$2g_{9/2} \to 3d_{5/2}$	6	−25.6	0.84
	4	33.7	0.84
	2	−37.3	0.84
$3d_{5/2} \to 1i_{11/2}$	8	14.4	0.82
	6	−9.8	0.81
	4	6.5	0.81
$2g_{9/2} \to 2g_{7/2}$	8	24.2	0.83
	6	−16.8	0.83
	4	12.2	0.82
	2	−5.5	0.82
$2g_{7/2} \to 1i_{11/2}$	8	5.2	0.80
	6	−8.6	0.79
	4	11.0	0.79
	2	−12.7	0.78
$2g_{9/2} \to 4s_{1/2}$	4	76.2	0.87
$4s_{1/2} \to 1i_{11/2}$	6	−14.9	0.84
$2g_{9/2} \to 3d_{3/2}$	6	−53.3	0.87
	4	27.3	0.86
$3d_{3/2} \to 1i_{11/2}$	6	−10.4	0.84
	4	16.4	0.83

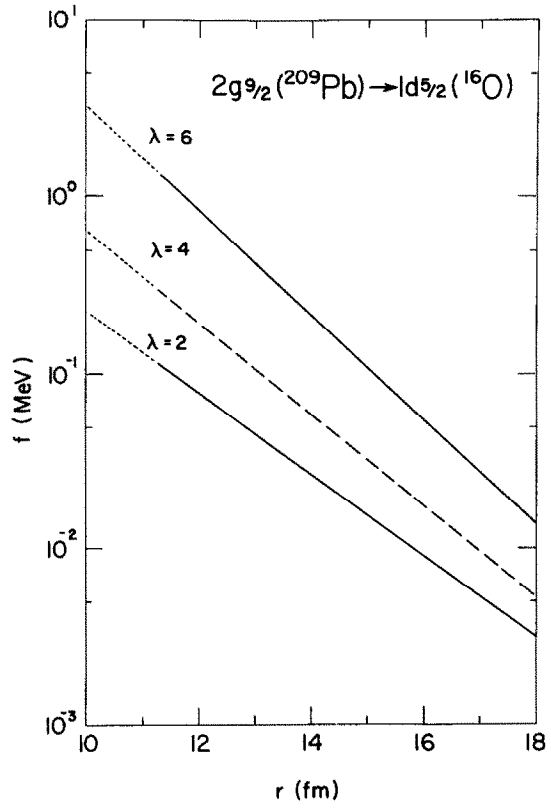

Fig. 3. Single-particle transfer form factors for the different multipolarities in the reaction $^{209}Pb(2g_{9/2})(^{16}O,^{17}O(1d_{5/2}))^{208}Pb$.

TABLE 2

Strength and diffuseness parameters of single-particle transfer form factors for $^{209}Pb(^{16}O,^{17}O)$ and $^{208}Pb(^{17}O,^{16}O)$

Transition	λ	F_0 [MeV]	a [fm]
$2g_{9/2} \rightarrow 1d_{5/2}$	6	−3.0	1.47
	4	0.6	1.68
	2	−0.2	1.88
$1d_{5/2} \rightarrow 1i_{11/2}$	8	5.4	1.40
	6	−0.2	1.65
	4	0.1	2.25
$2g_{9/2} \rightarrow 2s_{1/2}$	4	−2.3	1.67
$2s_{1/2} \rightarrow 1i_{11/2}$	6	2.3	1.70

fig. 1 are collected in table 1. The average diffuseness for these inelastic transitions is $a = 0.75$ fm.

Transfer reaction form factors connecting the $^{209}Pb(2g_{9/2})$ and $^{17}O(1d_{5/2})$ states are shown in fig. 3. Here the shapes for the different multipolarities are similar but the magnitudes increase with increasing angular momentum transfer. Notice the slower rate of decay as compared to the inelastic excitation form factors shown in fig. 2. The exponential parametrizations for all of the transfer form factors which contribute to the process $^{209}Pb(2g_{9/2}) \rightarrow {}^{17}O(nlj) \rightarrow {}^{209}Pb(1i_{11/2})$ are collected in table 2. Notice that the strength parameters are smaller than those for the single-particle excitations in table 1 but that the diffuseness values are about twice as large.

Using the results in tables 1 and 2 we construct the effective imaginary form factors for the $2g_{9/2} \rightarrow 1i_{11/2}$ transition according to the formula given at the end of subsect. 2.1. For these calculations we used a value of $\ddot{r}_0$ obtained with a head-on Coulomb trajectory for $^{16}O + {}^{208}Pb$ at a center-of-mass energy of 100 MeV. The

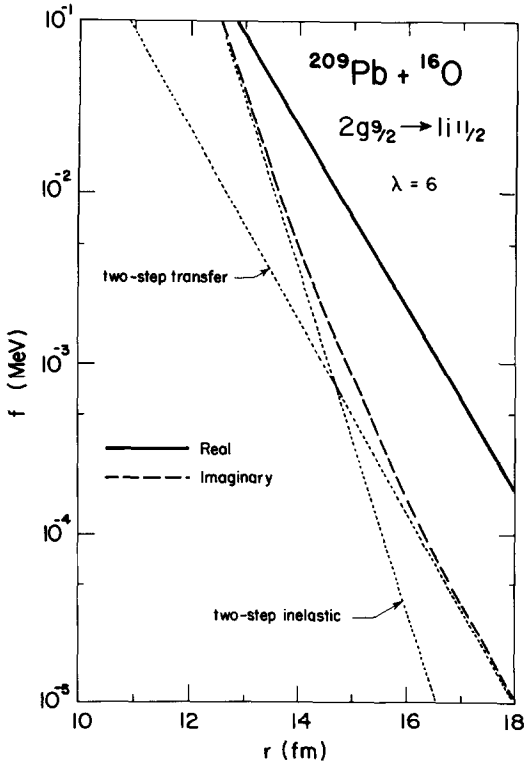

Fig. 4. Imaginary form factor for the $^{209}Pb(2g_{9/2})(^{16}O,^{16}O')^{209}Pb(1i_{11/2})$ $\lambda = 6$ transition (dashed curve) calculated from the two-step inelastic transitions of table 1 and the two-step transfer reactions of table 2. The corresponding contributions are shown separately. The solid curve is the direct real form factor.

results for the $\lambda = 6$ transfer is plotted in fig. 4. The contributions from the two-step inelastic and two-step transfer reactions are also shown separately and the real form factor for the direct excitation is given again for comparison.

These calculations clearly show how the transfer reactions dominate the imaginary form factor at large distances. Notice that the slope of the imaginary two-step transfer form factor is close to that of the direct real form factor. The contribution from inelastic transitions has a steeper slope but becomes strong only at smaller distances thus causing a shape change in the imaginary form factor. At large distances, $r \gtrsim 15$ fm, the ratio of the imaginary to the real form factor is approximately equal to 0.1.

These results are encouraging. A typical empirical ratio of imaginary to real form factors is about 0.2–0.5. On the other hand, this ratio has not been particularly well determined and our calculations are for a rather specialized problem. For instance, we would expect a relatively smaller contribution from inelastic excitation processes in the types of collective excitations which are usually analyzed.

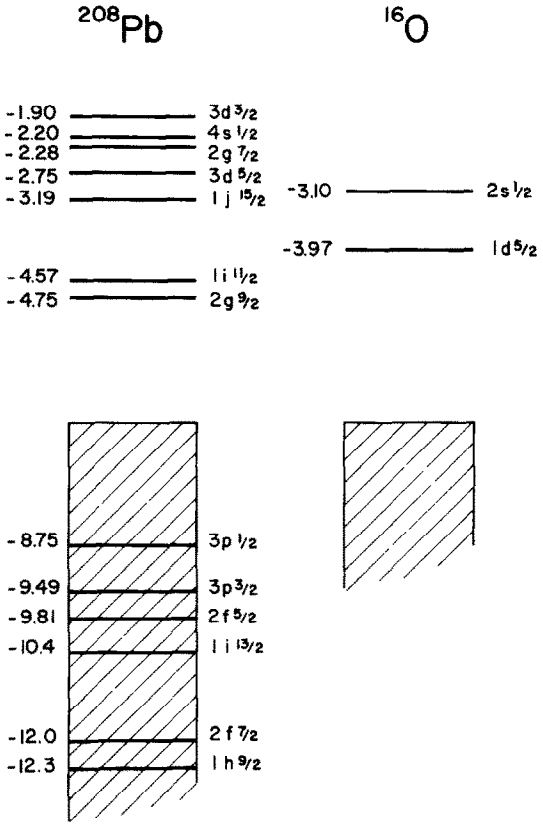

Fig. 5. Neutron particle and hole orbitals around the closed shells corresponding to ^{208}Pb and ^{16}O.

4.2. PARTICLE-HOLE EXCITATIONS

Eventually one would like to calculate imaginary form factors for collective excitations using RPA wave functions. At the present stage we have studied some typical particle-hole components of such wave functions which would occur in the $^{16}O + ^{208}Pb$ collision (see fig. 5). As we have mentioned, exciting particle-hole states is essentially equivalent to making single-particle excitations. However there is a physical difference in that the energies of the particle-hole states are usually larger. We also present the correction to the real form factor in this case. As we consider these particle-hole configurations to be components of collective excitations we only allow for two-step transfer processes in the calculations which follow.

We have first considered the neutron particle-hole configuration $(2g_{9/2}, (3p_{3/2})^{-1})$ coupled to angular momentum $\lambda = 3$ (fig. 5). This is the strongest component in the RPA wave function for the low-lying $^{208}Pb(3^-)$ state. The direct excitation form factor, the imaginary form factor resulting from the two-step transfers via ^{17}O, and

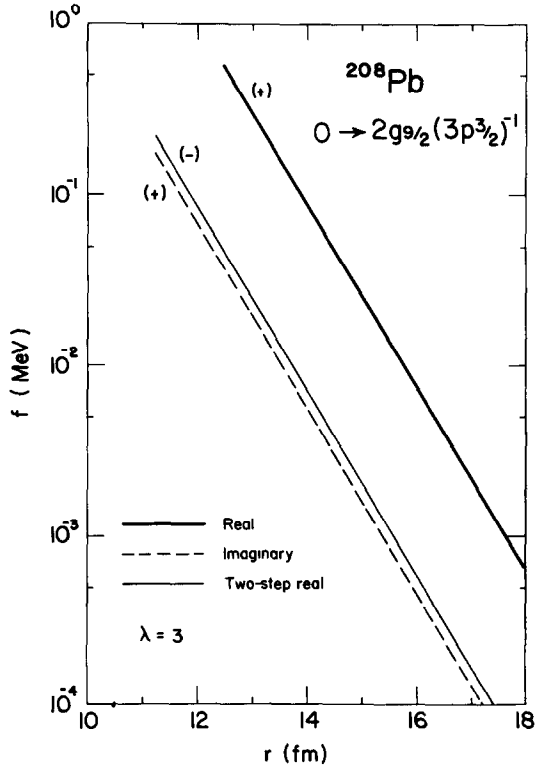

Fig. 6. Microscopic form factors for the particle-hole excitation $^{208}Pb(^{16}O, ^{16}O')^{208}Pb(2g_{9/2}(3p_{3/2})^{-1}; \lambda = 3)$. Indicated are the direct real form factor and the effective real and imaginary form factors calculated from two-step transfer reactions via the $1d_{5/2}$ and $2s_{1/2}$ states of ^{17}O.

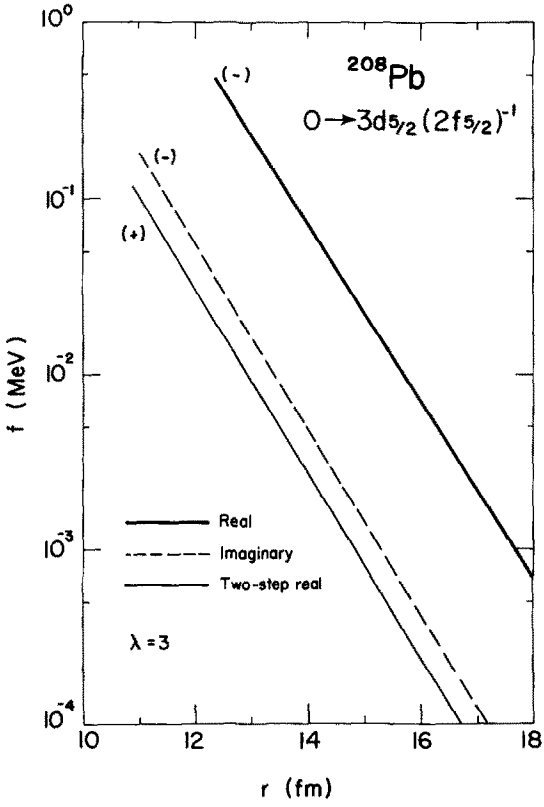

Fig. 7. Same as fig. 6 but for the particle-hole excitation $^{208}Pb(^{16}O,^{16}O')^{208}Pb(3d_{5/2}(2f_{5/2})^{-1};\ \lambda = 3)$.

the corresponding second-order contribution to the real form factor are shown in fig. 6. The excitation energy in this case is 4.7 MeV, whereas it was only 0.2 MeV in the example above. Nevertheless the ratio of real to imaginary form factors (0.1 at $r = 15$ fm) is similar to the previous calculation.

It is seen that the second-order correction to the real form factor is as large as the imaginary form factor. This is because the energies of the intermediate states do not lie at about half the excitation energy. The (positive) excitation energies of the first transfer reaction are larger than the (negative) energies of the second step resulting in a destructive contribution (see sect. 3).

We have repeated these calculations for the $(3d_{5/2},(2f_{5/2})^{-1};\ \lambda = 3)$ configuration which has a larger excitation energy (7 MeV). As shown in fig. 7, similar results are obtained. In particular the ratio of the imaginary to real form factors is practically the same. We have also obtained similar results when coupling the configurations to $\lambda = 5$.

In an RPA calculation the excitation amplitude of the low-lying collective state is built coherently from such individual particle-hole contributions. The present calcu-

lations indicate that the ratio of the real to imaginary coupling strengths for such collective excitations is more or less established already at the particle-hole excitation level.

5. Conclusions

In this work we have derived an explicit expression for the effective first-order inelastic excitation form factor which takes into account second-order inelastic and transfer reaction processes. It is seen that at large distances each second-order process adds constructively to the imaginary part of the form factor. The inelastic excitations give rise to relatively short-ranged imaginary form factors and are expected to make small contributions for collective excitations. In any case the transfer reactions should govern the long-range part of the imaginary form factor.

The microscopic expressions show how the main features of the usual macroscopic prescription can be understood. The imaginary coupling interaction should be approximately proportional to and of the same order of magnitude as the imaginary part of the optical potential in the tail region. The empirical diffuseness of the macroscopic imaginary form factor is explained by the fact that the product of two transfer reaction form factors decays like an inelastic excitation form factor.

The calculations carried out for specific single-particle excitations illustrate how the two-step transfer contributions dominate the imaginary form factor at large distances. They also give a reasonable order of magnitude for the ratio of imaginary to real form factors. It is interesting that the second-order contribution to the real form factor and the imaginary part have comparable strength; given the established formal analogy, a similar relation is to be expected between the imaginary component of the optical potential and the second-order contribution to the real part [5]). The results are found to be insensitive to the total excitation energy and total angular momentum transfer of the reactions studied. We are therefore encouraged that the widely used empirical prescription for the imaginary form factor can be understood in microscopic terms.

It is a pleasure to thank A. Winther for helpful discussions.

References

1) R.A. Broglia, C.H. Dasso, G. Pollarolo and A. Winther, Phys. Reports **48** (1978) 351
2) K. Alder and A. Winther, Electromagnetic excitation (North-Holland, Amsterdam, 1975)
3) G. Pollarolo, R.A. Broglia and A. Winther, Nucl. Phys. **A406** (1983) 369;
R.A. Broglia, G. Pollarolo and A. Winther, Nucl. Phys. **A361** (1981) 307
4) R.A. Broglia and A. Winther, Heavy ion reactions; Lecture notes, vol. 1, (Benjamin/Cummings, Reading, Mass., 1981) p. 254
5) C.H. Dasso, S. Landowne and G. Pollarolo, to be published